

Analytical vectorial structure of non-paraxial four-petal Gaussian beams in the far field

Xuewen Long^{a,b}, Keqing Lu^{a,*}, Yuhong Zhang^{a,b}, Jianbang Guo^{a,b}, and Kehao Li^{a,b}

^a*State Key Laboratory of Transient Optics and Photonics,*

Xi'an Institute of Optics and Precision Mechanics,

Chinese Academic of Sciences, Xi'an 710119, China

^b*Graduate school of Chinese Academy of Sciences, Beijing, 100039, China*

(Dated: August 16, 2021)

Abstract

The analytical vectorial structure of non-paraxial four-petal Gaussian beams(FPGBs) in the far field has been studied based on vector angular spectrum method and stationary phase method. In terms of analytical electromagnetic representations of the TE and TM terms, the energy flux distributions of the TE term, the TM term, and the whole beam are derived in the far field, respectively. According to our investigation, the FPGBs can evolve into a number of small petals in the far field. The number of the petals is determined by the order of input beam. The physical pictures of the FPGBs are well illustrated from the vectorial structure, which is beneficial to strengthen the understanding of vectorial properties of the FPGBs.

PACS numbers: 41.85.Ew, 42.25.Bs

Keywords: four-petal Gaussian beam, vectorial structure, far field

*Electronic address: keqinglu@opt.ac.cn

I. INTRODUCTION

Recently, a new form of laser beams called four-petal Gaussian beams (FPGBs) has been introduced and its properties of passing through a paraxial ABCD optical system have been studied [1]. Subsequently, the propagation properties of the FPGBs have attracted considerable interest due to its potential applications. Gao and Lü studied its vectorial non-paraxial propagation in free space based on vectorial Rayleigh-Sommerfeld diffraction integral formulas in 2006 [2]. In 2007, the propagation of four-petal Gaussian beams in turbulent atmosphere was investigated by Chu *et al* [3]. In 2008, Tang *et al* explored diffraction properties of four-petal Gaussian beams in uniaxially anisotropic crystal by virtue of the paraxially vectorial theory of beam propagation [4]. Yang *et al* reported the propagation of four-petal Gaussian beams in strongly nonlocal nonlinear media in the next year [5]. In the meanwhile, the vectorial structure of lots of beam with different patterns and polarized status is illustrated in the far field by means of vector angular spectrum method [6], which is a useful tool to resolve the Maxwell's equations, and stationary phase method [7, 8], which uses the asymptotic approximation approaching some kind of difficult integral. Based on these two methods mentioned above, Zhou studied analytical vectorial structure of Laguerre-Gaussian beam in the far field firstly [9]. Afterwards, Deng and Guo explored analytical vectorial structure of radially polarized light beams [10]. In 2008, Wu *et al* and Zhou *et al* investigated vectorial structure of hollow Gaussian beam almost in the same time [11, 12]. In fact, much work has been done with the vectorial structure of all kinds of beams in the far field [13]- [16].

It is well known that the paraxial approximation is no longer valid for beams with a large divergent angle or, especially, a small beam spot size that is comparable with the light wavelength [17]. Therefore, rigorous non-paraxial and vectorial treatments are necessary. We can approach non-paraxial propagation of beams in terms of vector angular spectrum method of electromagnetic field. According to vector angular spectrum method of electromagnetic field, the general solution of the Maxwell's equations is composed of the transverse electric (TE) term and the transverse magnetic (TM) term. In the far field, the TE and TM terms are orthogonal to each other and can be detached.

To the best of our knowledge, the research on the vectorial structure of non-paraxial four-petal Gaussian beam in the far field based on vector angular spectrum method and stationary phase method has not been reported elsewhere. In this paper, the far-field vectorial

properties of non-paraxial four-petal Gaussian beam have been studied by means of vector angular spectrum method and stationary phase method. Based on the analytical vectorial structure of the FPGBs, the energy flux distributions of TE term, TM term and the whole FPGBs are also investigated, respectively.

II. ANALYTICAL VECTORIAL STRUCTURE IN THE FAR FIELD

Let us consider a half space $z > 0$ filled with a linear homogeneous, isotropic, nonconducting medium characterized by electric permittivity ε and magnetic permeability μ . All the sources only lie in the domain $z < 0$. The electric field distribution is known at the boundary plane $z = 0$. For convenience of discussion, we consider a non-paraxial FPGBs with polarization in x direction, which propagates toward the half space $z \geq 0$ along the z axis. The initial transverse electric field distribution of the FPGBs at the $z = 0$ plane can be written by [1]

$$E_x(x, y, 0) = G_n \left(\frac{xy}{w_0^2} \right)^{2n} \exp \left(-\frac{x^2 + y^2}{w_0^2} \right), n = 1, 2, 3 \dots, \quad (1)$$

$$E_y(x, y, 0) = 0, \quad (2)$$

where n is the beam order of the FPGBs; G_n is a normalized amplitude constant associated with the order of n ; w_0 is the $1/e^2$ intensity waist radius of the Gaussian term. The time factor $\exp(-i\omega t)$ has been omitted in the field expression. Fig. 1 shows intensity distributions of four-petal Gaussian beams at the initial plane $z = 0$ for $n = 1, 5, 9$ and 13 , respectively. From Fig. 1, it can be seen that the intensity distributions is composed of four equal petals. The distance of small petals increases when beam order increases. Here, w_0 is taken by λ in the calculation, which is comparable with the wavelength. So, this is a non-paraxial problem.

In terms of Fourier transform, the vectorial angular spectrum of electric field at the $z = 0$ plane is expressed as [11]

$$A_x(p, q) = \frac{1}{\lambda^2} \int \int_{-\infty}^{\infty} E_x(x, y, 0) \exp[-ik(px + qy)] dx dy, \quad (3)$$

$$A_y(p, q) = \frac{1}{\lambda^2} \int \int_{-\infty}^{\infty} E_y(x, y, 0) \exp[-ik(px + qy)] dx dy, \quad (4)$$

where λ denotes the wave length in the medium related wave number by $k = 2\pi/\lambda$. Substituting Eqs. (1) and (2) into Eqs. (3) and (4), we find that

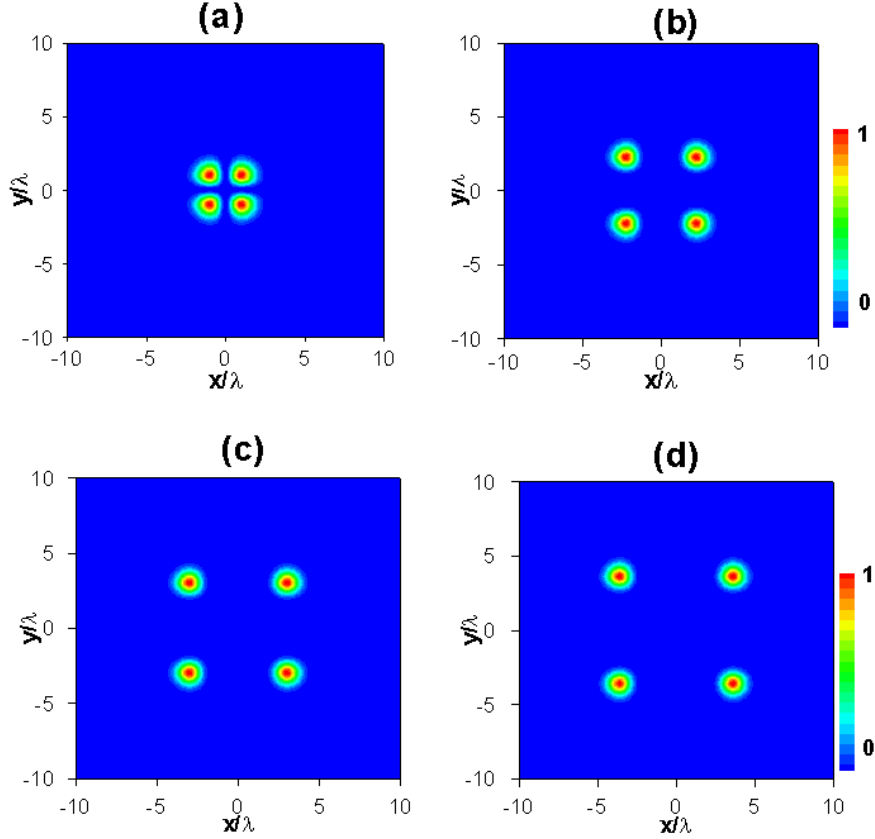


FIG. 1: (Color online) Normalized intensity distributions of FPGBs with different beam order n at $z = 0$ plane based Eq. (1). (a) $n = 1$, (b) $n = 5$, (c) $n = 9$, (d) $n = 13$.

$$A_x(p, q) = \frac{G_n}{\lambda^2} w_0^2 \left[\Gamma\left(n + \frac{1}{2}\right) \right]^2 {}_1F_1\left(n + \frac{1}{2}; \frac{1}{2}; -\frac{1}{4}k^2 p^2 w_0^2\right) \times {}_1F_1\left(n + \frac{1}{2}; \frac{1}{2}; -\frac{1}{4}k^2 q^2 w_0^2\right), \quad (5)$$

where ${}_1F_1(\cdot; \cdot; \cdot)$ denotes confluent hypergeometric function, $\Gamma(\cdot)$ denotes the Gamma function. It is well known that Maxwell's equations can be separated into transverse and longitudinal field equations and an arbitrary polarized electromagnetic beam, which is expressed in terms of vector angular spectrum, is composed of the transverse electric (TE) term and the transverse magnetic (TM) term, namely,

$$\vec{E}(\vec{r}) = \vec{E}_{TE}(\vec{r}) + \vec{E}_{TM}(\vec{r}), \quad (6)$$

$$\vec{H}(\vec{r}) = \vec{H}_{TE}(\vec{r}) + \vec{H}_{TM}(\vec{r}), \quad (7)$$

where

$$\begin{aligned}\vec{E}_{TE}(\vec{r}) = & \int \int_{-\infty}^{\infty} \frac{1}{p^2 + q^2} [qA_x(p, q) - pA_y(p, q)] (q\hat{e}_x - p\hat{e}_y) \\ & \times \exp(iku) dp dq, \end{aligned} \quad (8)$$

$$\begin{aligned}\vec{H}_{TE}(\vec{r}) = & \sqrt{\frac{\varepsilon}{\mu}} \int \int_{-\infty}^{\infty} \frac{1}{p^2 + q^2} [qA_x(p, q) - pA_y(p, q)] (p\gamma\hat{e}_x + q\gamma\hat{e}_y - b^2\hat{e}_z) \\ & \times \exp(iku) dp dq, \end{aligned} \quad (9)$$

and

$$\begin{aligned}\vec{E}_{TM}(\vec{r}) = & \int \int_{-\infty}^{\infty} \frac{1}{p^2 + q^2} [pA_x(p, q) + qA_y(p, q)] (p\hat{e}_x + q\hat{e}_y - \frac{b^2}{\gamma}\hat{e}_z) \\ & \times \exp(iku) dp dq, \end{aligned} \quad (10)$$

$$\begin{aligned}\vec{H}_{TM}(\vec{r}) = & -\sqrt{\frac{\varepsilon}{\mu}} \int \int_{-\infty}^{\infty} [pA_x(p, q) + qA_y(p, q)] \frac{1}{b^2\gamma} (q\hat{e}_x - p\hat{e}_y) \\ & \times \exp(iku) dp dq. \end{aligned} \quad (11)$$

$\vec{r} = x\hat{e}_x + y\hat{e}_y + z\hat{e}_z$ is the displacement vector and \hat{e}_x , \hat{e}_y , \hat{e}_z denote unit vectors in the x, y, z directions, respectively; $u = px + qy + \gamma z$; $b^2 = p^2 + q^2$; $\gamma = \sqrt{1 - p^2 - q^2}$, if $p^2 + q^2 \leq 1$ or $\gamma = i\sqrt{p^2 + q^2 - 1}$, if $p^2 + q^2 > 1$. The value of $p^2 + q^2 > 1$ corresponds to the evanescent wave which propagates along the boundary plane but decays exponentially along the positive z direction.

In the far field framework, the condition $k(x^2 + y^2 + z^2)^{1/2} \rightarrow \infty$ is satisfied due to z is big enough. Moreover the contribution of the evanescent wave to the far field can be ignored. By virtue of the method of stationary phase [7, 8, 11], the TE mode and the TM mode of the electromagnetic field can be given by

$$\begin{aligned}\vec{E}_{TE}(\vec{r}) = & -i \frac{G_n w_0^2}{\lambda} \frac{yz}{r^2 \rho^2} \left[\Gamma(n + \frac{1}{2}) \right]^2 {}_1F_1 \left(n + \frac{1}{2}; \frac{1}{2}; -\frac{1}{4} k^2 \frac{x^2}{r^2} w_0^2 \right) \\ & \times {}_1F_1 \left(n + \frac{1}{2}; \frac{1}{2}; -\frac{1}{4} k^2 \frac{y^2}{r^2} w_0^2 \right) \exp(ikr) (y\hat{e}_x - x\hat{e}_y), \end{aligned} \quad (12)$$

$$\begin{aligned}\vec{H}_{TE}(\vec{r}) = & -i \sqrt{\frac{\varepsilon}{\mu}} \frac{G_n w_0^2}{\lambda} \frac{yz}{r^3 \rho^2} \left[\Gamma(n + \frac{1}{2}) \right]^2 {}_1F_1 \left(n + \frac{1}{2}; \frac{1}{2}; -\frac{1}{4} k^2 \frac{x^2}{r^2} w_0^2 \right) \\ & \times {}_1F_1 \left(n + \frac{1}{2}; \frac{1}{2}; -\frac{1}{4} k^2 \frac{y^2}{r^2} w_0^2 \right) \exp(ikr) \\ & \times (xz\hat{e}_x + yz\hat{e}_y - \rho^2\hat{e}_z), \end{aligned} \quad (13)$$

and

$$\begin{aligned}\vec{E}_{TM}(\vec{r}) = & -i\frac{G_n w_0^2}{\lambda} \frac{x}{r^2 \rho^2} \left[\Gamma(n + \frac{1}{2}) \right]^2 {}_1F_1 \left(n + \frac{1}{2}; \frac{1}{2}; -\frac{1}{4}k^2 \frac{x^2}{r^2} w_0^2 \right) \\ & \times {}_1F_1 \left(n + \frac{1}{2}; \frac{1}{2}; -\frac{1}{4}k^2 \frac{y^2}{r^2} w_0^2 \right) \exp(ikr) \\ & \times (xz\hat{e}_x + yz\hat{e}_y - \rho^2\hat{e}_z),\end{aligned}\tag{14}$$

$$\begin{aligned}\vec{H}_{TM}(\vec{r}) = & i\sqrt{\frac{\varepsilon}{\mu}} \frac{G_n w_0^2}{\lambda} \frac{x}{r \rho^2} \left[\Gamma(n + \frac{1}{2}) \right]^2 {}_1F_1 \left(n + \frac{1}{2}; \frac{1}{2}; -\frac{1}{4}k^2 \frac{x^2}{r^2} w_0^2 \right) \\ & \times {}_1F_1 \left(n + \frac{1}{2}; \frac{1}{2}; -\frac{1}{4}k^2 \frac{y^2}{r^2} w_0^2 \right) \exp(ikr) \\ & \times (y\hat{e}_x - x\hat{e}_y),\end{aligned}\tag{15}$$

where $\rho = \sqrt{x^2 + y^2}$; $r = \sqrt{x^2 + y^2 + z^2}$. Eqs. (12)- (15) are analytical vectorial expressions for the TE and TM terms in the far field and constitute the basic results in this paper. From Eqs. (12)- (15), we find that

$$\vec{E}_{TE}(\vec{r}) \cdot \vec{E}_{TM}(\vec{r}) = 0,\tag{16}$$

$$\vec{H}_{TE}(\vec{r}) \cdot \vec{H}_{TM}(\vec{r}) = 0.\tag{17}$$

According to Eqs. (16) and (17), the TE and TM terms of FPGBs are orthogonal to each other in the far field.

III. ENERGY FLUX DISTRIBUTIONS IN THE FAR FIELD

The energy flux distributions of the TE and TM terms at the $z = \text{const}$ plane are expressed in terms of the z component of their time-average Poynting vector as

$$\langle S_z \rangle_{TE} = \frac{1}{2} \text{Re}[\vec{E}_{TE}^* \times \vec{H}_{TE}]_z,\tag{18}$$

$$\langle S_z \rangle_{TM} = \frac{1}{2} \text{Re}[\vec{E}_{TM}^* \times \vec{H}_{TM}]_z,\tag{19}$$

where the Re denotes real part, and the asterisk denotes complex conjugation. The whole energy flux distribution of the beam is a sum of the energy flux of TE mode and TM mode, namely,

$$\langle S_z \rangle = \langle S_z \rangle_{TE} + \langle S_z \rangle_{TM},\tag{20}$$

Substituting Eqs. (12)- (15) into Eqs. (18)- (19) yields

$$\begin{aligned} \langle S_z \rangle_{TE} = & \frac{1}{2} \sqrt{\frac{\varepsilon}{\mu}} \frac{G_n^2 w_0^4}{\lambda^2} \frac{y^2 z^3}{r^5 \rho^2} \left[\Gamma\left(n + \frac{1}{2}\right) \right]^4 {}_1F_1 \left(n + \frac{1}{2}; \frac{1}{2}; -\frac{1}{4} k^2 \frac{x^2}{r^2} w_0^2 \right)^2 \\ & \times {}_1F_1 \left(n + \frac{1}{2}; \frac{1}{2}; -\frac{1}{4} k^2 \frac{y^2}{r^2} w_0^2 \right)^2, \end{aligned} \quad (21)$$

$$\begin{aligned} \langle S_z \rangle_{TM} = & \frac{1}{2} \sqrt{\frac{\varepsilon}{\mu}} \frac{G_n^2 w_0^4}{\lambda^2} \frac{x^2 z}{r^3 \rho^2} \left[\Gamma\left(n + \frac{1}{2}\right) \right]^4 {}_1F_1 \left(n + \frac{1}{2}; \frac{1}{2}; -\frac{1}{4} k^2 \frac{x^2}{r^2} w_0^2 \right)^2 \\ & \times {}_1F_1 \left(n + \frac{1}{2}; \frac{1}{2}; -\frac{1}{4} k^2 \frac{y^2}{r^2} w_0^2 \right)^2, \end{aligned} \quad (22)$$

Therefore, the whole energy flux distribution of FPGs in the far field is given by

$$\begin{aligned} \langle S_z \rangle = & \frac{1}{2} \sqrt{\frac{\varepsilon}{\mu}} \frac{G_n^2 w_0^4}{\lambda^2} \frac{z}{r^3 \rho^2} \left(\frac{y^2 z^2}{r^2} + x^2 \right) \left[\Gamma\left(n + \frac{1}{2}\right) \right]^4 \\ & \times {}_1F_1 \left(n + \frac{1}{2}; \frac{1}{2}; -\frac{1}{4} k^2 \frac{x^2}{r^2} w_0^2 \right)^2 \\ & \times {}_1F_1 \left(n + \frac{1}{2}; \frac{1}{2}; -\frac{1}{4} k^2 \frac{y^2}{r^2} w_0^2 \right)^2. \end{aligned} \quad (23)$$

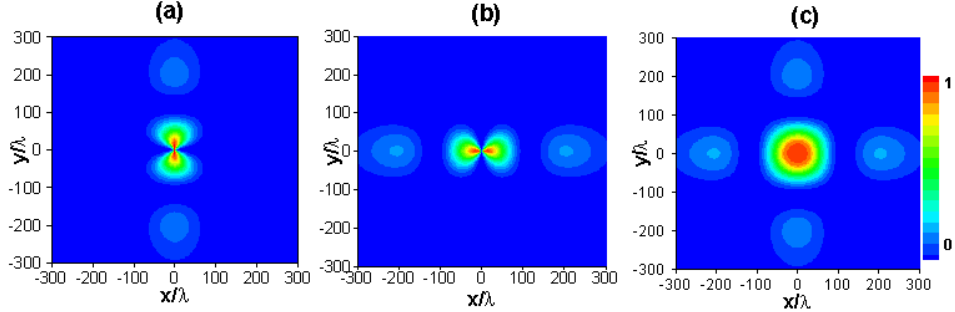


FIG. 2: (Color online) Normalized energy flux distributions of FPGs at the plane $z = 500\lambda$ for beam order $n = 1$. (a) The TE term, (b) The TM term, (c) The whole beam.

The normalized energy flux distributions of the TE term, the TM term and the FPGs at the plane $z = 500\lambda$ for different beam order $n = 1, 5, 9, 13$ versus x/λ and y/λ are illustrated by Figs. 2- 5. The used parameter is $w_0 = \lambda$. As can be seen from Figs. 2- 5, the FPGs split into a number of small petals in the far field, which differs from its initial four-petal shape. The FPGs with beam order n is not a pure mode, which can be regarded as a superposition of n^2 two dimensional Hermite-Gaussian modes [1], and different modes

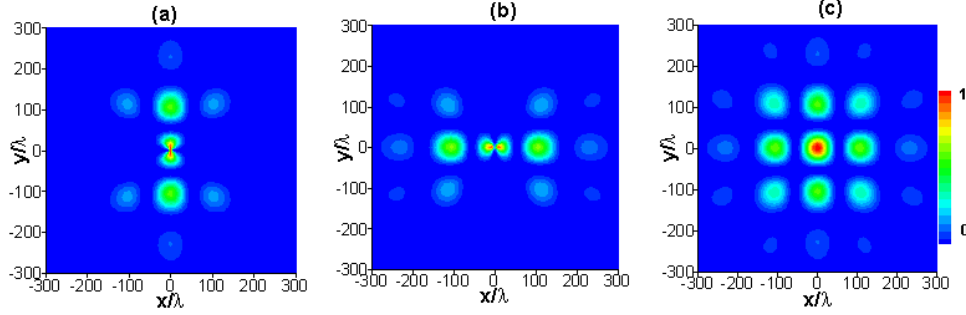


FIG. 3: (Color online) Normalized energy flux distributions of FPGBs at the plane $z = 500\lambda$ for beam order $n = 5$. (a) The TE term, (b) The TM term, (c) The whole beam.

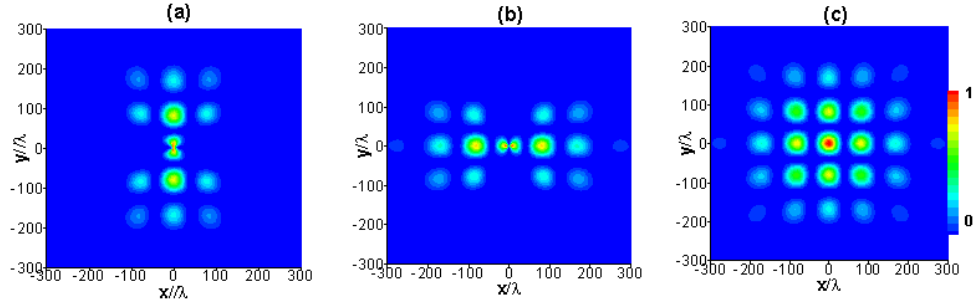


FIG. 4: (Color online) Normalized energy flux distributions of FPGBs at the plane $z = 500\lambda$ for beam order $n = 9$. (a) The TE term, (b) The TM term, (c) The whole beam.

evolve differently within the same propagation distance. The overlap and interference in propagation between different modes result in the propagation properties of the FPGBs in the far field. Furthermore, the number of petals is determined by the parameter n . The number of petals in the far field gradually increases when the parameter n increases, which has potential applications in micro-optics and beam splitting techniques, etc. Note that diameter of the central beam spot decreases when beam order n increases. This phenomenon has been discussed in some previous researches [1]- [3].

IV. CONCLUSIONS

In summary, the vectorial structure of the non-paraxial four-petal Gaussian beam in the far field is expressed in the analytical form by using the vector angular spectrum method and the stationary phase method. The electric field and the magnetic field of the four-petal

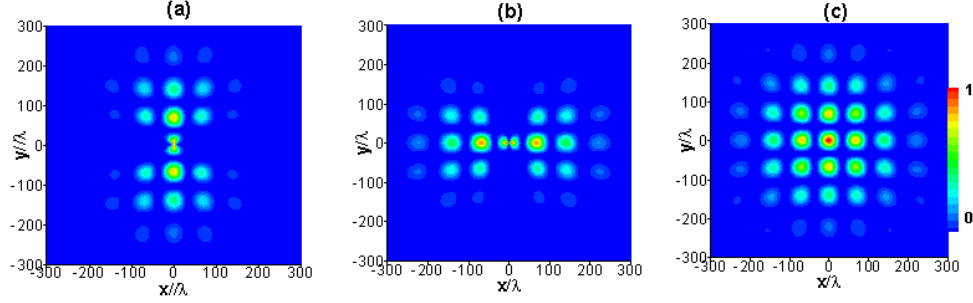


FIG. 5: (Color online) Normalized energy flux distributions of FPGs at the plane $z = 500\lambda$ for beam order $n = 13$. (a) The TE term, (b) The TM term, (c) The whole beam.

Gaussian beam is decomposed into two mutually orthogonal terms, i.e., TE term and TM term. Based on the analytical vectorial structure of FPGs, the energy flux distributions of the TE term, the TM term and the whole beam of FPGs are derived in the far-field and are illustrated by numerical examples. The number of petals and diameter of the central beam spot in the far field are determined by the beam order n . The potential applications of the FPGs are deserved investigation. This work is important to understand the theoretical aspects of vector FPGs propagation.

Acknowledgments

This research was supported by the National Natural Science Foundation of China (Grant No.10674176). The author is beneficial from the discussion with the author of Ref. [11].

-
- [1] K. Duan and B. Lü, Opt. Commun. **261**, 327 (2006).
 - [2] Z. Gao and B. Lü, Chin. Phys. Lett. **23**, 2070 (2006).
 - [3] X. Chu, J. Liu and Y. Wu, Chin. Phys. Lett. **25**, 485 (2008).
 - [4] B. Tang, Y. Jin, M. Jiang and X. Jiang, Chin. Opt. Lett. **6**, 779 (2008).
 - [5] Z. Yang, D. Lu, D. Deng, S. Li, W. Hu and Q. Guo, Opt. Commun. **283**, 595 (2010).
 - [6] Rosario Martínez-Herrero and Pedro M. Mejías, J. Opt. Soc. Am. A **18**, 1678 (2001).
 - [7] L. Mandel and E. Wolf, *Optical Coherence and Quantum Optics* (Cambridge University Press, Cambridge, 1995).

- [8] M. Born and E. Wolf, *Principles of Optics*, 7th Edition (Cambridge University Press, Cambridge, 1999).
- [9] G. Zhou, Opt. Lett. **31**, 2616 (2006).
- [10] D. Deng and Q. Guo, Opt. Lett. **32**, 2711 (2007).
- [11] G. Wu, Q. Lou and J. Zhou, Opt. Express **16**, 6417 (2008).
- [12] G. Zhou, X. Chu and J. Zheng, Opt. Commun. **281**, 5653 (2008).
- [13] G. Zhou, Y.Z. Ni and Z. Zhang, Opt. Commun. **272**, 32 (2007).
- [14] G. Zhou and F. Liu, Opt. Laser Technol. **40**, 302 (2008).
- [15] H. Tang, X. Li, G. Zhou and K. Zhu, Opt. Commun. **282**, 478 (2009).
- [16] G. Zhou, J. Opt. Soc. Am. B **26**, 2386 (2009).
- [17] Nemoto Shojiro, Appl. Opt. **29**, 1940 (1990).